Do subglacial bedforms comprise a size and shape continuum?

Jeremy C. Ely [a,*], Chris D. Clark [a], Matteo Spagnolo [b], Chris R. Stokes [c], Sarah L. Greenwood [d], Anna L.C. Hughes [e], Paul Dunlop [f], Dale Hess [g]

[a] Department of Geography, University of Sheffield, Sheffield S10 2TN, UK
[b] School of Geosciences, University of Aberdeen, Aberdeen AB24 3UF, UK
[c] Department of Geography, Durham University, Durham DH1 3LE, UK
[d] Department of Geological Sciences, Stockholm University, Stockholm SE-106 91, Sweden
[e] Department of Earth Science, University of Bergen and Bjerknes Centre for Climate Research, Bergen N-5020, Norway
[f] School of Geography and Environmental Sciences, Ulster University, Coleraine BT52 1SA, UK
[g] Department of Earth and Environmental Sciences, The University of Rochester, Rochester, NY 14627, United States

ABSTRACT

Understanding the evolution of the ice-bed interface is fundamentally important for gaining insight into the dynamics of ice masses and how subglacial landforms are created. However, the formation of the suite of landforms generated at this boundary — subglacial bedforms — is a contentious issue that is yet to be fully resolved. Bedforms formed in aeolian, fluvial, and marine environments either belong to separate morphological populations or are thought to represent a continuum of forms generated by the same governing processes. For subglacial bedforms, a size and shape continuum has been hypothesised, yet it has not been fully tested. Here we analyse the largest data set of subglacial bedform size and shape measurements ever collated (96,900 bedforms). Our results show that flutes form a distinct population of narrow bedforms. However, no clear distinction was found between drumlins and megascale glacial lineations (MSGLs), which form a continuum of subglacial lineations. A continuum of subglacial ribs also exists, with no clear size or shape distinctions indicating separate populations. Furthermore, an underreported class of bedform with no clear orientation to ice flow (quasi-circular bedforms) overlaps with the ribbed and lineation continua and typically occurs in spatial transition zones between the two, potentially merging these three bedform types into a larger continuum.

Crown Copyright © 2016 Published by Elsevier B.V. This is an open access article under the CC BY license (http://creativecommons.org/licenses/by/4.0/).

1. Introduction

The interface between moving water, air, or ice and unconsolidated sediment is often populated by undulating landforms, collectively referred to as bedforms (e.g., Allen, 1968; Wilson, 1973; Aario, 1977; Rose and Letzer, 1977). Rather than being individuals, bedforms commonly occur in swathes or fields: configurations which cover large portions of Earth's deserts, river beds, and ocean floors (e.g., Costello and Southard, 1981; Amos and King, 1984; Carling, 1999), as well as the surfaces of extraterrestrial bodies (Cutts and Smith, 1973; Kargel and Strom, 1992; Radebaugh et al., 2008). The abundance of subglacial bedforms on deglaciated terrain (e.g., Aylsworth and Shilts, 1989; Ottesen et al., 2005; Greenwood and Clark, 2008; Larter et al., 2009; Trommelen and Ross, 2010; McHenry and Dunlop, 2015), their emergence from receding ice margins (Johnson et al., 2010), and their repeated detection by geophysical surveys of contemporary ice-sheet beds (Rooney et al., 1987; Smith et al., 2007; King et al., 2009) indicates that they are a key component of the subglacial environment, where

processes that regulate ice flow occur (Alley et al., 1986; Engelhardt and Kamb, 1998; Kleman and Glasser, 2007). Elucidating the genesis of subglacial bedforms is an important goal in geomorphology and for understanding ice dynamics.

In addition to their composition, the morphological properties of bedforms provide constraints for hypotheses and models of their formation (e.g., Jackson, 1975; Clark et al., 2009; Worman et al., 2013). Fluvial, aeolian, and marine bedforms can form distinct, often hierarchical, populations (Allen, 1968). In deserts, for example, discrete populations of bedforms are found, increasing in size from ripples to dunes then draas (Wilson, 1973; Lancaster, 1988). Conversely, bedforms can also belong to populations within which there are no clear size distinctions, forming size and shape continua [e.g., aeolian ripples (Ellwood et al., 1975), aeolian dunes (Lancaster, 2013, p. 159), and subaqueous dunes (Ashley, 1990)]. For flutes, drumlins, megascale glacial lineations (MSGLs), and ribbed moraines, whether they form separate distinct morphological populations or form a single continuous size and shape population with no natural breaks (i.e., a size and shape continuum) is unclear.

Subglacial bedforms are often subdivided and named on the basis of perceived distinctions in scale and morphology. Commonly, subglacial

bedforms that form aligned with ice-flow direction are divided into drumlins, MSGLs, and flutes (Fig. 1); whilst ribbed moraines and megaribs form transverse to flow direction (Fig. 1; Greenwood and Kleman, 2010; Klages et al., 2013). Quasi-circular bedforms, which have no clear orientation to ice-flow direction, are less frequently studied but have been previously noted (Hill, 1973; Markgren and Lassila, 1980; Bouchard, 1989; Smith and Wise, 2007; Greenwood and Clark, 2008). Beyond this, a wealth of further nomenclature exists (e.g., megaflutes, fluting, megadrumlins, and minor ribbed, Blatnick, Rogen, and Niemsel moraines).

Despite the array of terms applied to the varieties comprising subglacial bedforms, a long-standing hypothesis is that they actually belong to a continuum of size and shape (Aario, 1977; Rose and Letzer, 1977; Rose, 1987). This 'continuum hypothesis' was originally based upon observations of spatial transitions between subglacial bedform types and orientations along the direction of ice flow, suggesting a single continuum of form stretching from ribbed moraine, through quasi-circular forms, to drumlins (Aario, 1977; Markgren and Lassila, 1980; Punkari, 1984). However, subsequent work on the continuum hypothesis has focussed solely upon flow-aligned subglacial bedforms (e.g., Rose, 1987; Stokes et al., 2013b). Furthermore, the relatively recent discovery of 'megascale' subglacial bedforms (Clark, 1993; Greenwood and Kleman, 2010) might imply a distinct variety of bedform rather than end-members of a continuum. Morphological studies often focus upon previously labelled categories of subglacial bedforms [e.g. drumlins in Clark et al. (2009) and Maclachlan and Eyles (2013); ribbed moraines in Hättestrand (1997) and Dunlop and Clark (2006b); MSGL in Spagnolo et al. (2014a)]. A comprehensive study that looks at all landform types together to compare and contrast their size and shape is missing. Here, we present and analyse a data set of 96,900 size and shape measurements of subglacial bedforms from numerous locations, spanning the range of types in the literature, in order to investigate whether there is a continuum of subglacial bedforms or whether separate size and shape populations exist. Note that we do not consider bedforms composed purely of bedrock (e.g., whalebacks, roche moutonnées, megagrooves), nor do we consider hybrid forms such as crag and tails, as they are often regarded as different from subglacial

bedforms created in sediment (e.g., Dionne, 1987; Stokes et al., 2011; Lane et al., 2015).

2. Data and methods

2.1. Data

A database of 96,900 mapped subglacial bedforms was compiled from previous studies and additional mapping, which was conducted using standard remote sensing techniques (Table 1). A variety of reported bedform morphologies from a wide range of sites were chosen from the literature (Fig. 2; Table 1). Mapped bedforms were grouped by locality and reported type (i.e., as reported in previous studies) so that further analysis could ascertain the similarities or differences between these types. At each location, the highest resolution remote sensing data available were used to map and derive landforms metrics (Table 2). Only data with resolution higher than 30 m were used, as measurements of bedform length and width derived from coarser resolution data have been shown to misrepresent subglacial bedform size and shape (Napieralski and Nalepa, 2010). Each bedform is represented in our data set as a smooth polygon, manually digitised directly into a geographic information system (GIS) around the break of slope on hill-shaded digital elevation models illuminated from multiple directions (Smith and Clark, 2005; Hughes et al., 2010). On satellite imagery, landforms are detectable as a change in vegetation and/or soil moisture (e.g., Spagnolo et al., 2014a). Automated mapping techniques (e.g., Saha et al., 2011; Maclachlan and Eyles, 2013) were avoided as they require predefinition of parameters such as shape and scale and thus would introduce bias into our results.

2.2. Methods

The length (L) and width (W) of each mapped polygon was estimated via Euler's approximation for an ellipse (Clark et al., 2009). A limitation of this approximation is that it slightly underestimates the length (and overestimates the width) of highly elongate or irregular polygons, but this error is insignificant compared to the size of
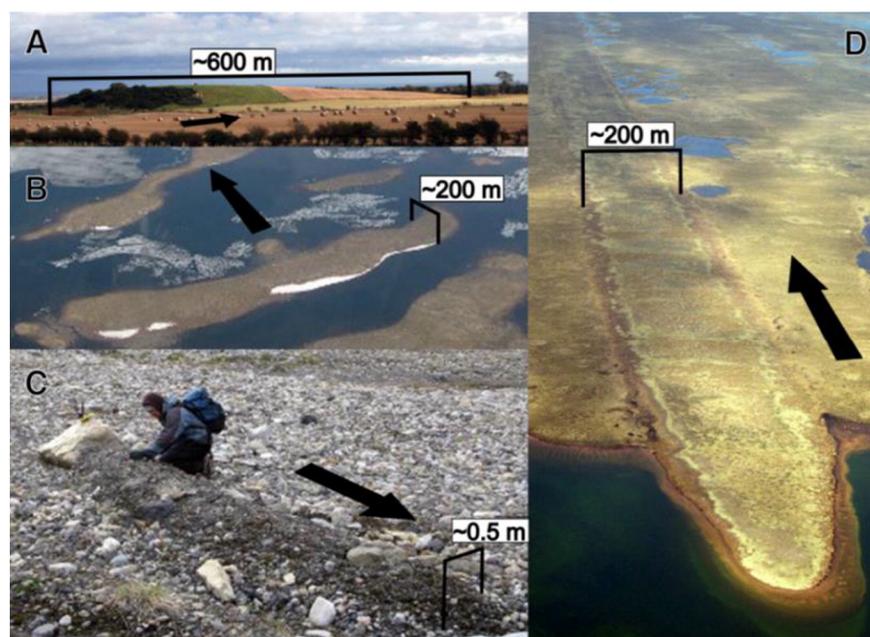

Fig. 1. Different types of subglacial bedform and their orientation to ice-flow direction (denoted by black arrow). Scales are approximate. (A) A drumlin in NE England. These streamlined hills are typically 250–1000 m along-flow and 120–300 m across-flow (Clark et al., 2009). (B) Transverse ridges, termed ribbed moraine, in Nunavut, Canada, typically 300–1200 m across-flow and 150–300 m along-flow (Hättestrand and Kleman, 1999). (C) A flute formed parallel to ice-flow direction, Svalbard. Note the accumulation of sediment in the lee of a boulder. (D) A MSGL in Nunavut, Canada. MSGLs typically are 100–200 m across-flow and 1–9 km along-flow (Spagnolo et al., 2014a) but have been reported to be much longer (e.g., 180 km, Andreassen et al., 2008). All photographs from www.shef.ac.uk/drumlins.

Table 1
Location of mapped subglacial bedforms; all bedforms have previously been described in the literature. Where mapping was not available from the original study a '#' denotes that further mapping was conducted at a previously described site.

Reported bedform type (number of bedforms)	Location	Central coordinates (decimal degrees)	Number of bedforms	Data set	Study describing site (# denotes mapping has not previously been analysed)	Location number
Drumlins (n = 42,495)	Britain	54.069, 2.258	30,304	NEXTMap DEM	Hughes et al. (2010)	1
	New York State, USA	44.830, −75.268	5650	USGS NED	Hess and Briner (2009)	2
	Alta, Norway	69.476, 23.139	1638	Landsat ETM+	Spagnolo et al. (2010)	3
	Ungava Bay, Quebec, Canada	57.176, −67.299	5903	Landsat ETM+	Spagnolo et al. (2010)	4
MSGL (n = 31,668)	Cameron Hills, Alberta, Canada	59.950, −117.826	581	SPOT	Brown et al. (2011) #	5
	Dubawnt Lake, Nunavut, Canada	64.171, −100.415	17,038	Landsat ETM+	Stokes et al. (2013b)	6
	Eskimo Bay, Nunavut, Canada	61.387, −94.829	4499	SPOT	Clark (1993) #	7
	Great Bear Lake, NWT, Canada	64.454, −122.069	1260	SPOT	Winsborrow et al. (2004) #	8
	Haldane Ice Stream, NWT, Canada	67.008, −121.299	489	SPOT	Winsborrow et al. (2004) #	9
	Liard Ice Stream, NWT, Canada	61.217, −121.701	340	SPOT	Brown et al. (2011) #	10
	Great Slave Lake, NWT, Canada	61.703, −116.576	784	SPOT	Brown et al. (2011) #	11
	Payne Bay, Quebec, Canada	59.618, −70.430	531	SPOT	This study #	12
	M'Clintock Channel Ice Stream, Canada	72.743, −105.753	2796	Landsat ETM+	Storrar and Stokes (2007) #	13
	West James Bay Ice Stream	54.478, −87.280	3350	SPOT	Clark (1993) #	14
Quasi-circular bedforms (n = 1955)	Ireland	53.723, −7.803	1955	Landmap DEM, SRTM, Landsat ETM+	Greenwood and Clark (2008)	15
Flutes (n = 664)	Skeiðarajökull, Iceland	63.977, −17.219	101	NERC ARSF aerial photography	Waller et al. (2008) #	16
	Breiðamerkurjökull, Iceland	64.071, −16.327	131	NERC ARSF Aerial Photography	Evans and Twigg (2002) #	17
	Conwaybreen, Svalbard	78.994, 12.486	432	NERC ARSF aerial photography	This study #	18
Ribbed moraine (n = 18,384)	Ireland	53.723, −7.803	5464	Landmap Dem, SRTM, Landsat ETM+	Greenwood and Clark (2008)	19
	Lac Naococane, Quebec, Canada	52.972, −70.921	501	Landsat	Dunlop and Clark (2006a) #	20
	St. Lawrence Valley, New York	44.831, −75.268	921	USGS NED	Carl (1978) #	21
	Lake Rogen, Sweden	62.328, 12.394	3,357	Landsat ETM+	Dunlop and Clark (2006b) #	22
	Ungava Bay, Quebec, Canada	59.618, −70.430	7582	Landsat ETM+	Dunlop and Clark (2006b) #	23
	Great Slave Lake, NWT, Canada	61.703, −116.576	559	SPOT	Brown et al. (2011) #	24
Mega subglacial ribs (n = 733)	Keewatin, Canada	64.171, −100.415	733	Landsat ETM+ and SPOT	Greenwood and Kleman (2010)	25

the bedforms (Clark et al., 2009) and typically is less than 3%. These polygon measurements were then converted into *a*-axis (distance down-ice) and *b*-axis (distance across-ice) measurements according to bedform orientation to ice flow (Fig. 3). For near-circular bedforms, bedform *a*-axis and *b*-axis were manually measured within a GIS using regional ice-flow patterns as an indicator of flow alignment (Fig. 3). Elongation ratio, often used as a proxy for shape (e.g., Rose, 1987; Clark et al., 2009; Dowling et al., 2015), was simply measured as *a*-axis divided by *b*-axis.

Testing the subglacial bedform continuum hypothesis requires the detection and definition of populations within our data set. If the variously-named types of bedforms are found to vary continuously in size and shape such that, for example, a large drumlin is the same as a small MSGL, then a size and shape continuum between them exists (Fig. 4A and B). When plotted on a scatter graph, this would show a single continuous data cloud, or cluster (Fig. 4B). On the contrary, if the derived metrics reveal gaps or jumps in scale or shape then they are better interpreted as discrete phenomena (Fig. 4C and D), leading to the rejection of the continuum hypothesis. In this case, a scatter graph of bedform metrics would show several distinct clusters (Fig. 4D). Several

approaches are taken here to assess the degree to which separate populations, or clusters, can be detected within our data set.

The human eye is an excellent tool for detecting clusters (Jain, 2010). As such, our first attempt at detecting clusters in our data set was to plot the data and visually assess clustering qualitatively. That said, different interpreters may see different clusters. Thus, in an effort to make our analysis more objective and quantitative we employed the density-based clustering algorithm DBSCAN (Ester et al., 1996) using the package 'fpc' in R statistical software. No clustering algorithm or technique is perfect because no objective definition of a cluster exists (Estivill-Castro, 2002). However, DBSCAN was chosen as it requires no predefinition of the number of expected clusters within a data set; hence it requires no prior categorisation of bedforms into separate populations. The algorithm requires two input parameters: the window size (ε) and the minimum number of points within a cluster (*MinPts*). In order to define dense regions (clusters) within a point cloud, DBSCAN creates a window at each point and determines which points are sufficiently reachable from each other in order to warrant definition as a cluster (Ester et al., 1996). Core points are deemed reachable if there are more than *MinPts* within the search radius of ε from that point,
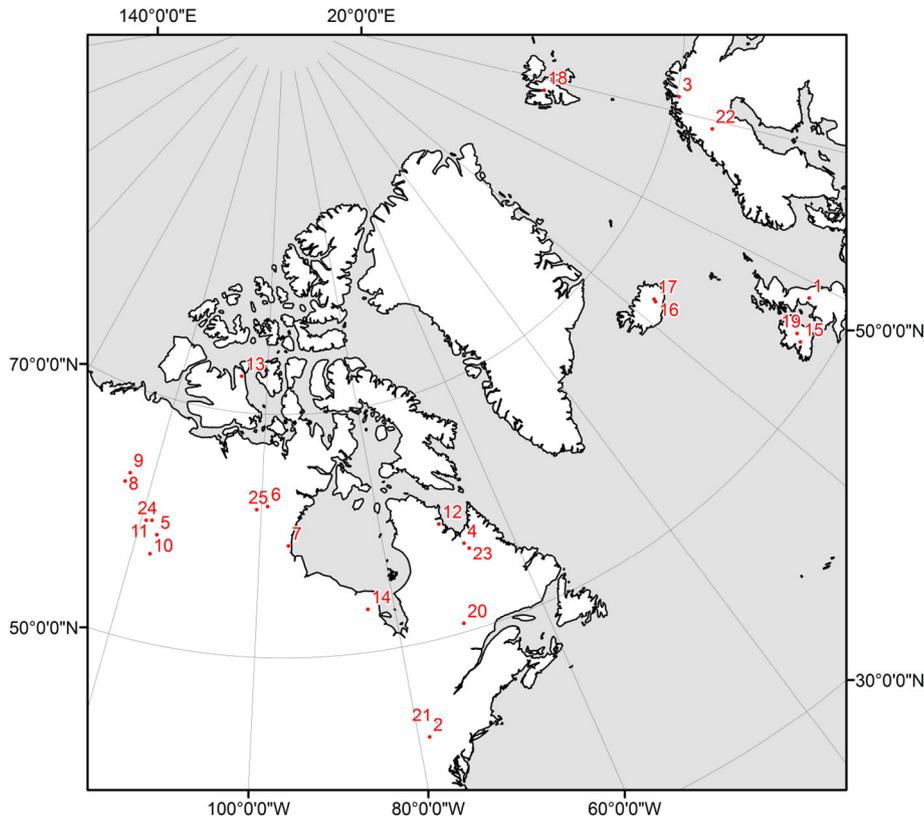
Fig. 2. Location of mapped subglacial bedforms. Numbers refer to Table 1.

and are included within the cluster owing to point density. Additionally, points are also deemed cohesive with the cluster if a core point is within the radius of ε. If neither of these criteria are met, the point is deemed to be outside of the cluster or is left unclustered. Sensitivity analysis of cluster-definition to window size (ε) was run from $\varepsilon = 1.0$ to $\varepsilon = 0.01$ with steps of $\varepsilon = 0.01$. The sensitivity of minimum points per cluster (MinPts) was also tested at values of 10, 50, and 100. The DBSCAN procedure was only conducted on the independent variables of length and width, elongation being derived from the two.

A second approach based on a direct, visual assessment of the degree of overlap between assigned bedform category metrics was also applied (Table 1). In covariance plots of the measured variables (e.g., length vs. width), the density of observations per category were calculated and contoured. Here, the highest density contour contained 75% of the observations, the middle 95%, and the lowest 99%. The degree of overlap between adjacent categories was then evaluated in order to test the validity of frequently used bedform nomenclature.

3. Results

The size and shape of all 96,900 subglacial bedforms in our data set are displayed in Fig. 5. The most striking aspect is that data are concentrated into a narrow range of values. When plotted on linear axes (Fig. 5A), there appears to be two clouds of data which merge toward the origin of the plot. Larger bedforms (>10,000 m) are less frequent in our data set, but plot as extensions of the same data clouds rather than forming separate clusters. Due to the skew imposed by these large values, data was also plotted on a logarithmic scale (Fig. 5B–D). At first order, two clusters of data are visually discernible: a small cloud of narrow and elongate bedforms aligned with flow direction, and a much larger cloud comprising the remaining bedforms (Fig. 5D). Within this larger cloud, density variations occur, perhaps recording three populations that (in places) merge and overlap, or maybe this is a single cluster that has been incompletely sampled. Within the larger cloud, these subclusters exhibit ellipsoid scatters with apparent trends (red ellipses in Fig. 5D), with bedforms with a larger a-axis than b-axis following a separate trajectory to transverse bedforms. Bedforms with no clear orientation (i.e., circular) fall between these two groups.

To assess the degree to which separate populations are quantitatively distinctive, the density-based clustering algorithm (DBSCAN) was used with an extensive sensitivity analysis (results are summarised in Fig. 6). At the extremes of the window size parameter (ε), the algorithm groups the data into inappropriately sized clusters. When ε is large, the window size is such that the whole data set is seen as a single cluster (Fig. 5A). When ε is small, either numerous small clusters or no clusters at all are detected because of an insufficient search radius (Fig. 6O). The

Table 2
Data type and source for the mapping described in Table 1.

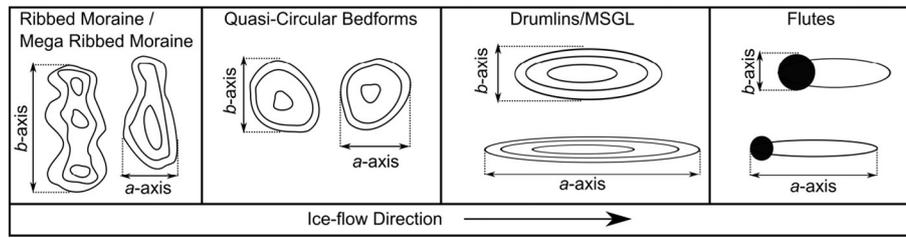| Data set	Type of data	Horizontal resolution (m)	Source
NEXTMap Great Britain™	DEM	5	http://arsf.nerc.ac.uk/
USGS NED	DEM	10 m	http://ned.usgs.gov/
Landsat ETM +	Imagery	15 pan-chromatic, 30 colour	http://earthexplorer.usgs.gov/
SPOT	Imagery	10 pan-chromatic, 20 colour	http://geobase.ca/
Landmap DEM	DEM	25	http://landmap.ac.uk/
NERC ARSF aerial photography	Imagery	0.15	http://arsf.nerc.ac.uk/
SRTM	DEM	30	http://earthexplorer.usgs.gov/

Fig. 3. Schematic of derived bedform axes.

most common result is that two clusters are detected (Fig. 6B–F, K, L, and N). These two clusters occur in the same positions as the first-order visual clustering (Fig. 5D). The larger cluster is not separated when the search window size parameter is adjusted from 0.5 to 0.06 (Fig. 6H–J). Beyond this, the larger cloud is separated into two clusters, one with bedforms aligned with flow direction and another with bedforms transverse to flow (Fig. 6K–N). For only a very small parameter space, DBSCAN distinguishes subglacial bedforms with no clear orientation with flow direction from flow-aligned and flow-transverse bedforms (Fig. 6M). Our results were found to be insensitive to the minimum number of points parameter (*MinPts*).

When each bedform's previously determined category was considered, the group of small bedforms that were distinguished visually (Fig. 5) and by DBSCAN (Fig. 6B–F), are revealed to be those that are commonly known as flutes (Figs. 7 and 8). The distinguishing factor of flutes is their *b*-axis, which is much smaller than for all other subglacial bedforms (Fig. 7), and has a narrow range and small measures of variance (Table 3). Overlap occurs between all other categories of bedform, as shown by the intersection of density contours belonging to adjacent categories (Fig. 7) and the frequency distribution of their measured metrics (Fig. 8). The strongest overlap occurs between drumlins and MSGLs, which for all parameter combinations occurs between 75% contours. The median *b*-axis, and the 10th and 90th percentiles of the drumlin and MSGL categories are remarkably similar (Table 3), indicating a consistency between the two groups. This contributes to the clustering of drumlins and MSGL together, visually and in DBSCAN (Figs. 5 and 6). The elongation ratio of ribbed moraines and megaribs is also similar, with low coefficients of variation (Table 3). This indicates a

similar shape. The size range of quasi-circular bedforms is much narrower compared to all other subglacial bedforms, except for flutes. Additionally, the coefficient of variation for their size metrics is small, hence their selective positioning on Fig. 5. The category of quasi-circular bedforms may contain bedforms some might categorise as either drumlins or ribbed moraines. However, the mean elongation ratio of 1.07 (Table 3) and the high density of data on Figs. 5, 6, 7, and 8 where the elongation ratio is 1 clearly indicates the existence of near-circular forms.

To assess if there are any systematic controls on bedform metrics from their geographic location, Fig. 9 plots the outlines of the data at each locality shown in Table 1. No single location plots separately to the others, with all locations showing multiple overlap with other areas.

4. Discussion

4.1. Is there a subglacial bedform size and shape continuum, several continua, or are they separate phenomena?

The number of populations or clusters, and therefore the number of continua, within our data set depends, to some extent, upon the interpretation of Figs. 5, 7, and 8, as well as the parameters chosen for DBSCAN (Fig. 6). However, a consistent result is that flutes plot separately to all other subglacial bedforms (Figs. 5–9), forming a distinct population. Given their smaller size, flutes could only be mapped from aerial photography (Tables 1 and 2), rather than digital terrain models or satellite images, but we do not interpret their separation to be a consequence of higher resolution imagery being used for mapping. This
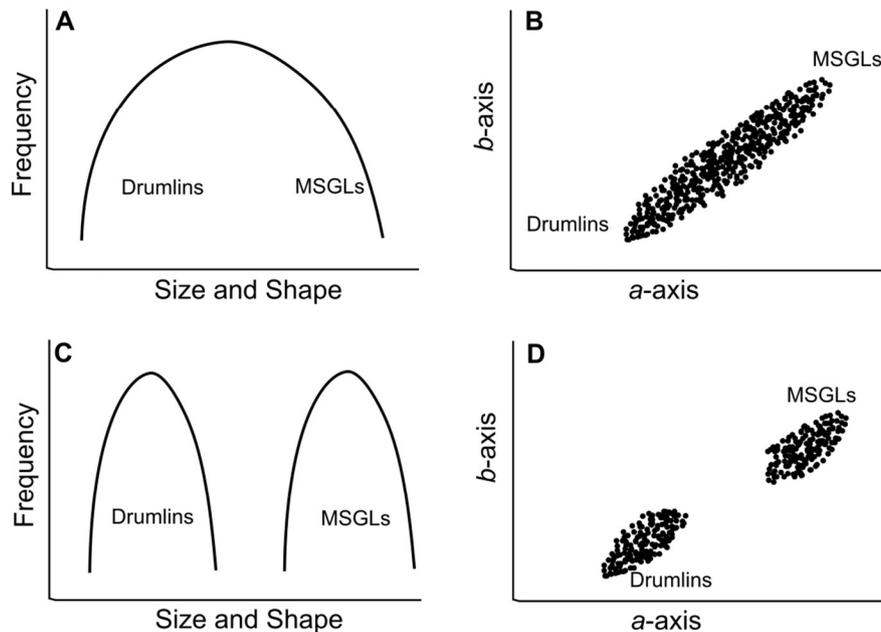

Fig. 4. Schematic of how a continuum (A and B) or different populations (C and D) may be detected in our data set. If a continuous sequence in the size and shape of bedforms exists, e.g., between drumlins and MSGLs (A), then a scatter plot of their metrics would show a single cluster. If separate size and shape populations occur (C), then separate clusters would be shown on a scatter plot (D).
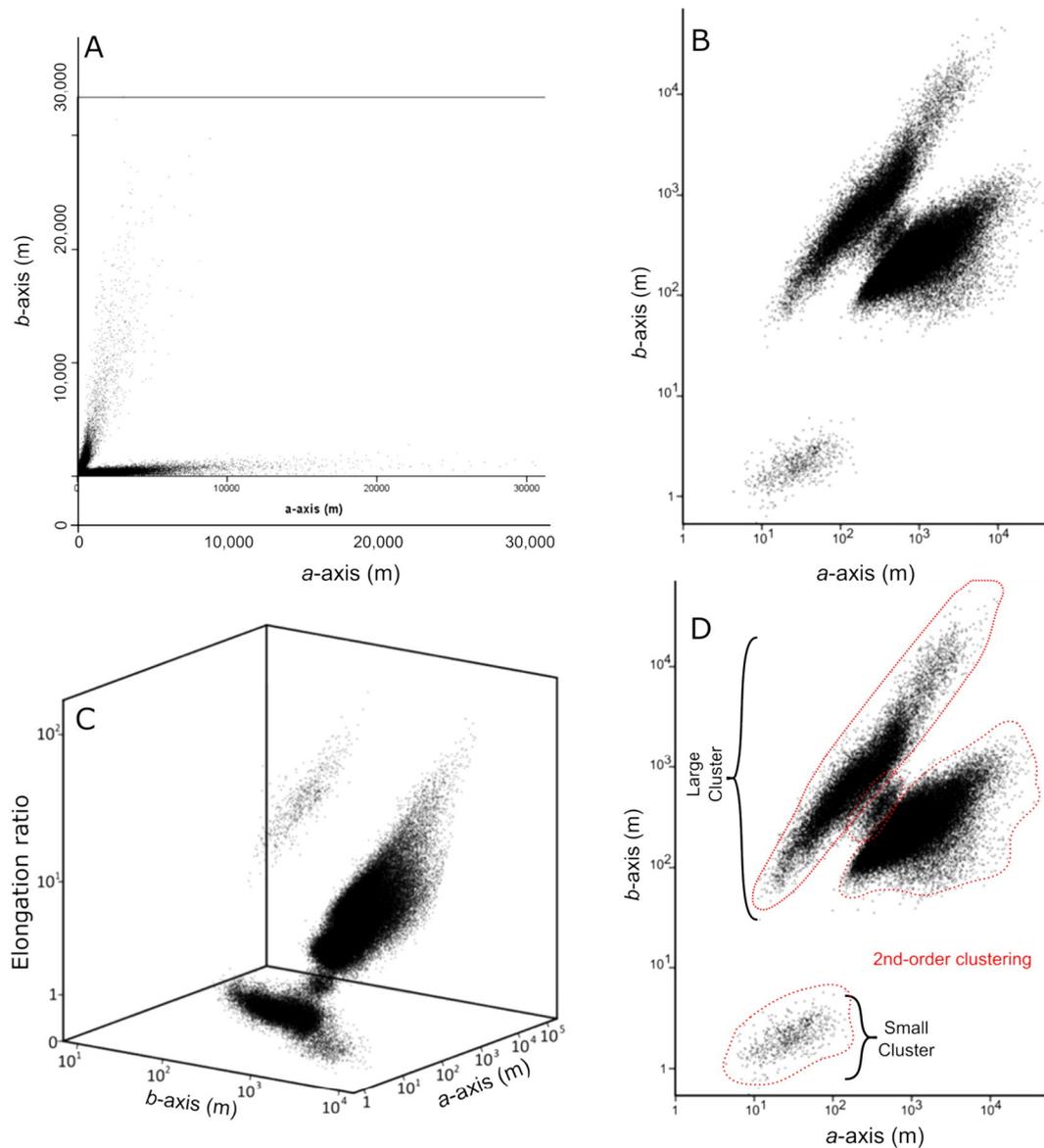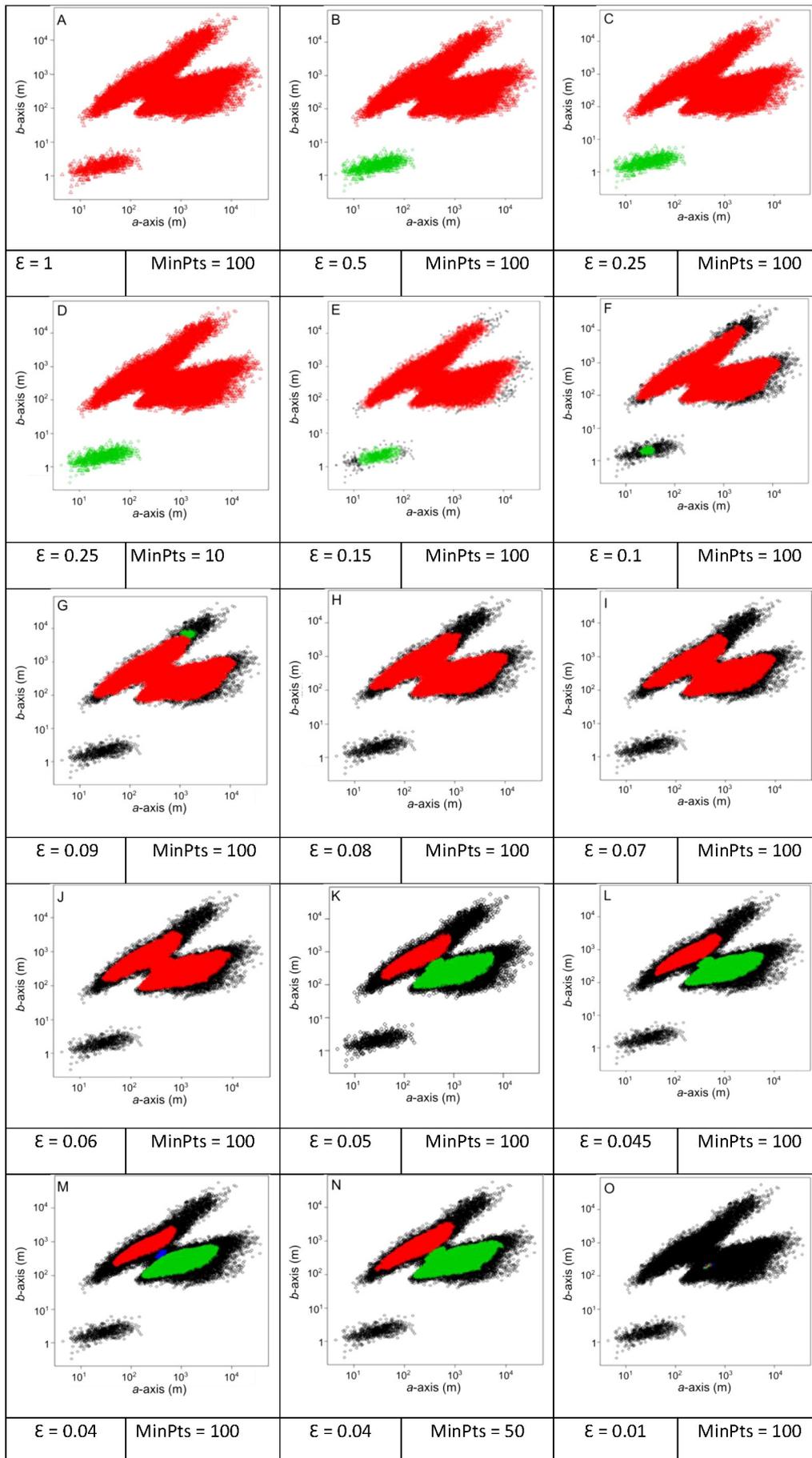
Fig. 5. The size and shape of all 96,900 subglacial bedforms, paying no regard to their nomenclature. (A) Plot of *a*-axis (down-flow) and *b*-axis (across flow) dimensions. (B) The same dimensions, plotted on log–log axes. (C) Combined plot of *a*-axis, *b*-axis and elongation ratio (*a/b*). Although elongation ratio is dependent upon *a* and *b* axes, it is plotted for visualisation purposes. (D) Two possible qualitative (visual) interpretations of clusters. Perhaps the data reveals just two clusters, or on closer inspection it might be possible to distinguish four. See text for further details.

interpretation is supported by observations of flutes that reach over 1.5 km long (exceeding the length of many drumlins) whilst maintaining their narrow width (Kjær et al., 2006). Flutes are often found superimposed on top of drumlins (e.g., Boulton, 1987; Hart, 1995; Waller et al., 2008), emphasising the scale difference between the two. We therefore interpret flutes to be morphologically distinct to all other subglacial bedforms, forming a group of narrow and elongate subglacial bedforms. Thus, a clear difference exists in scale between flutes and other subglacial bedforms. This is consistent with previous suppositions and interpretations (Boulton, 1976; Rose, 1987; Clark, 1993).

Aside from flutes, it is difficult to distinguish separate populations of bedforms that are elongated with ice-flow direction. A consistency in *b*-axis lengths and a lack of any stepwise jump in *a*-axis lengths between drumlins and MSGLs means that these two categories of flow-aligned bedforms were never separated by any combination of parameters in our quantitative analysis (Fig. 6). They display the highest level of overlap on Figs. 7 and 8. We therefore concur with previous work using a smaller data set (Stokes et al., 2013b) that drumlins and MSGL form a size and shape continuum of subglacial lineations.

Ribbed moraines and megascale ribs also possess overlapping size and shape metrics (Figs. 7 and 8), and were only partially separated by one combination of DBSCAN parameters (Fig. 6G), which may be a consequence of a smaller sample of mega-ribbed moraines. Both populations have a consistent elongation ratio of ≈ 0.3 (Table 3). We find no grounds to suggest different morphological populations of ribbed moraines, as suggested elsewhere (e.g., Hättestrand, 1997), as there is no clear break or stepwise relationship in the metrics to indicate separate size and shape categories. Furthermore, putatively different types and scales of subglacial ribs often display close spatial relationships (Greenwood and Kleman, 2010), and have been observed to occur in potentially evolutionary sequences (Markgren and Lassila, 1980). Therefore, we propose that ribbed moraines and mega-ribs form a size and shape continuum of transverse subglacial bedforms that can be called subglacial ribs.
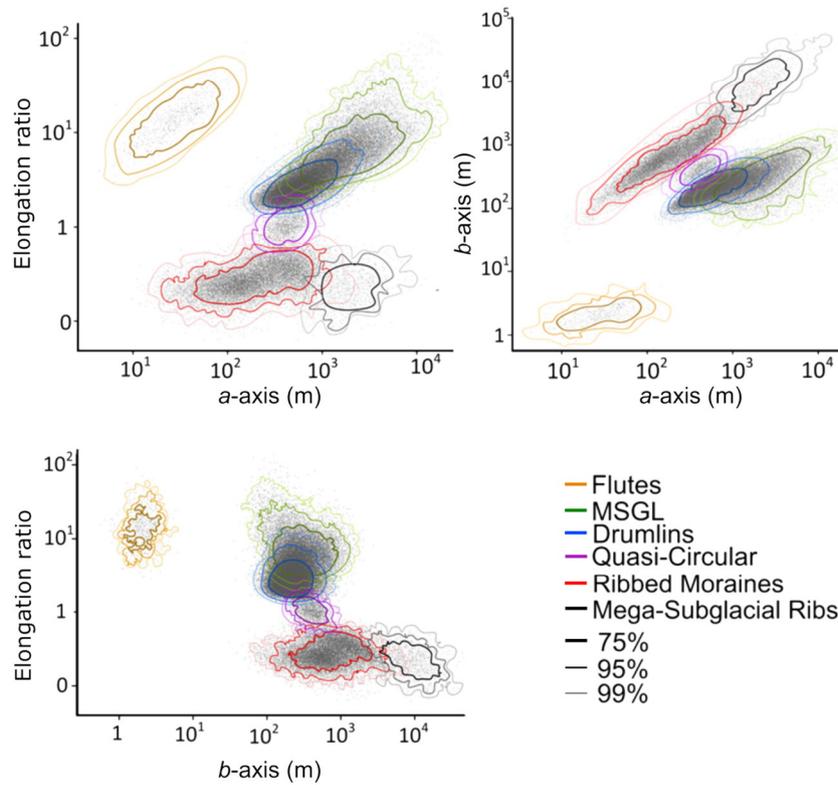
Fig. 7. Density contour plots to assess the degree of separation and overlap between named bedform types. Flutes consistently plot separately to all other bedform types, whilst overlap (*a*-axis, *b*-axis plot) occurs between other subglacial bedform types. Most notably, this overlap occurs between drumlins and MSGL (overlapping 75% contours) and between ribbed moraine and megasubglacial ribs (overlapping 90% contours). Quasi-circular bedforms overlap with ribbed moraine (90% contours) and drumlin (75%) contours. Note that elongation ratio is derived from length and width. However, it is plotted against its components here for illustrative purposes.

The existence of quasi-circular bedforms that overlap with drumlins and ribbed moraines (Figs. 5, 7, and 8) raises the possibility of a single bedform continuum comprising ribs to quasi-circular forms to lineations (e.g., Aario, 1977). All three are often categorised as one cluster by DBSCAN (Fig. 6B–J). When they are split into separate clusters by the quantitative analyses (Fig. 6K–N) it may be a consequence of a genuine difference in the shape and scale of subglacial ribs and lineations (Fig. 5D) and/or a small sample size of quasi-circular forms (Table 1). The bridging between ribbed moraines and drumlins provided by quasi-circular bedforms only occurs within a narrow range of *a*- and *b*-axis lengths, centred around 450 m (Figs. 5 and 8).

Quasi-circular bedforms — such as the Blattnick moraine of Markgren and Lassila (1980), the mammillary hills of Aario (1977), the circular forms noted by Knight et al. (1999), and the ovoid forms noted by Smith and Wise (2007) — are often reported in transition zones between ribbed moraines and drumlins. Quasi-circular forms were most notable in several locations across the bed of the Irish-ice sheet (Greenwood and Clark, 2008). Given their potential importance, further examples of quasi-circular bedforms were sought and are shown in Fig. 10. These examples illustrate how they occur in gradual down-ice transitions between subglacial ribs and lineations and sometimes superimposed upon subglacial ribs. Since subglacial bedforms are often assigned a label based upon flow orientation, perhaps quasi-circular forms have been confusing to identify and classify and are more common than is reported in the literature. As they may form an

important link between subglacial ribs and lineations, further work on quasi-circular bedforms is required.

4.2. Controls on the size and shape of subglacial bedforms

A correspondence between bedform size and shape and the flow characteristics of the geomorphic agent is often invoked for aeolian, fluvial, and marine bedforms (Allen, 1968; Rubin and Ikeda, 1990; Reffet et al., 2010). Similar links have been sought for subglacial bedforms (e.g., Rose and Letzer, 1977). Several lines of evidence that suggest that subglacial bedform size and shape is primarily determined by properties of the overlying ice mass. Firstly, bedforms within a flowset usually have a similar size, shape, and alignment to flow direction (Clark, 1999). Thus, different flow events, with different glaciological properties, produce different bedform morphologies. Secondly, bedforms are often observed to evolve gradually along former ice flow trajectories. Such evolutionary sequences can take the form of increases in the elongation of lineations (e.g., Ó Cofaigh et al., 2002; Stokes and Clark, 2002; Briner, 2007; Stokes et al., 2013b) or a switch from ribs to drumlins (e.g., Fig. 8; Aario, 1977; Aylsworth and Shilts, 1989; Dyke et al., 1992; Knight et al., 1999; Dunlop and Clark, 2006b). Both of these situations have been interpreted to indicate ice acceleration along flow, particularly in ice-stream settings (Aario, 1977; Hart, 1999; Ó Cofaigh et al., 2002; Stokes and Clark, 2002; Briner, 2007; Stokes et al., 2013a). Support for this is found from modern ice streams where drumlins have been observed beneath the onset zone

Fig. 6. DBSCAN sensitivity analysis to assess how many clusters exist using different parameter settings. Red, green, and blue indicate different clusters. Black points are disregarded by the clustering algorithm as being outside of any cluster caused by a lack of density and cohesiveness with other points. The most common result is that two clusters are detected (B, C, D, E, and F): narrow elongate bedforms and a larger cluster comprising of the remaining data. This occurs when $\varepsilon = 0.5–0.1$, and $MinPts = 10–100$ (B–F). For $\varepsilon = 0.09–0.06$ (G–J), the smaller cluster is not detected, but the large cluster remains. When $\varepsilon = 0.05–0.045$, clusters distinguish between flow alignment (K). At $\varepsilon = 0.04$ and $MinPts = 100$, a further small cluster between flow alignments is detected (blue in 'M'). Yet, a slight change in parameter values alters this result (N). When ε is too large, the whole data set is considered a cluster (A), or when ε is too small, no clusters or clusters of an inappropriate size are detected (O). (For interpretation of the references to colour in this figure legend, the reader is referred to the web version of this article.)
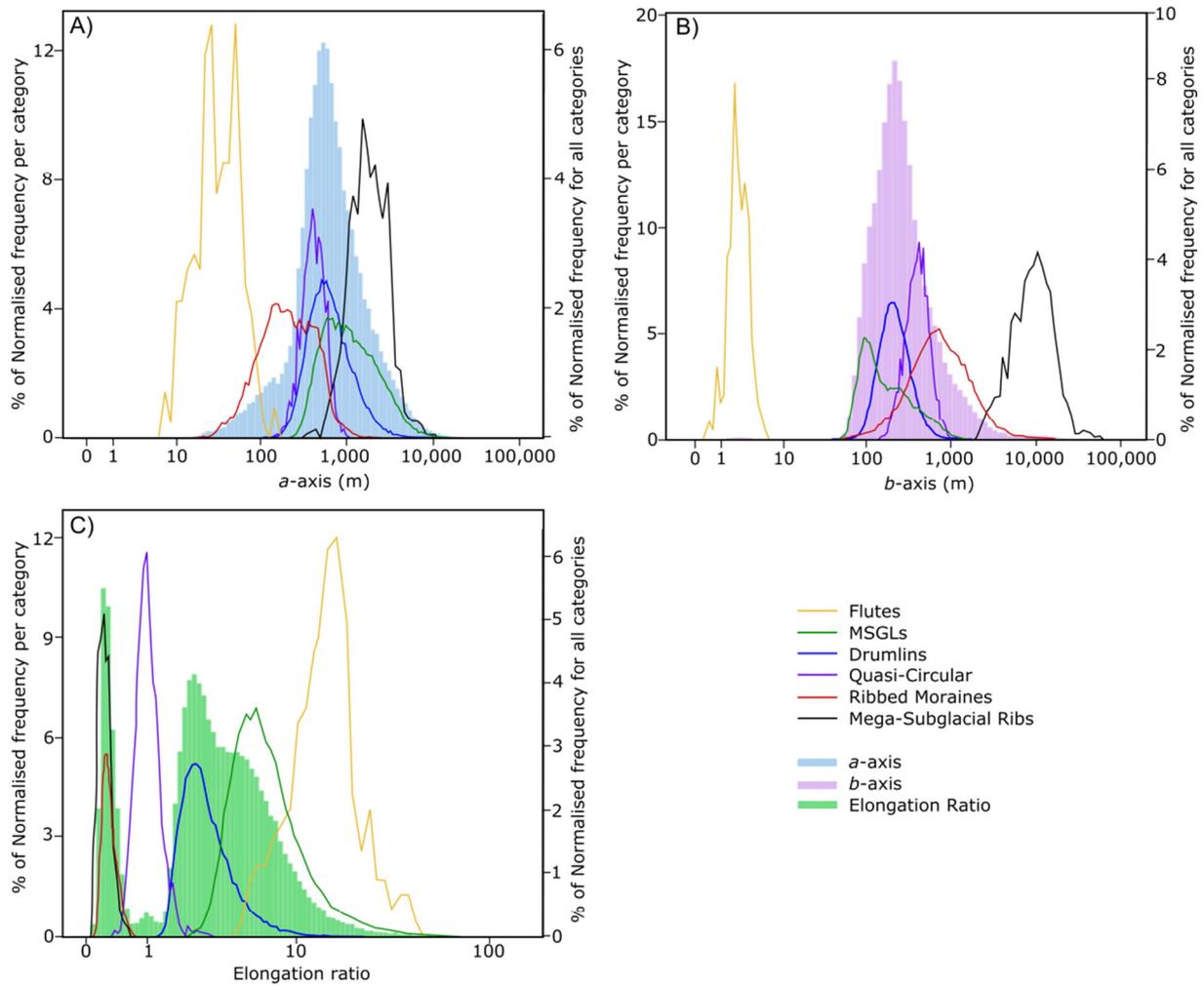
Fig. 8. Frequency distributions for (A) *a*-axis, (B) *b*-axis, and (C) elongation ratio. In each case, the probability distribution function of each bedform is plotted, normalised to the total population of their respective category in order to permit comparisons. This is plotted on the primary y-axis. The histograms (in solid colours) show the distribution of the whole population, plotted against the secondary y-axis.

of Rutford Ice Stream (King et al., 2007) and MSGLs farther down-flow where ice velocity is higher (King et al., 2009). Subglacial ribs can also be found in evolutionary sequences (Markgren and Lassila, 1980; Greenwood and Kleman, 2010), suggesting a gradual change in boundary

conditions, potentially induced by ice-flow properties. Thirdly, bedform morphology conforms strongly to glaciological variables at the ice-sheet scale (Greenwood and Clark, 2010). At the local scale, lithological, sedimentological, and topographical differences across a bedform field may

Table 3
Summary statistics of subglacial bedform categories.

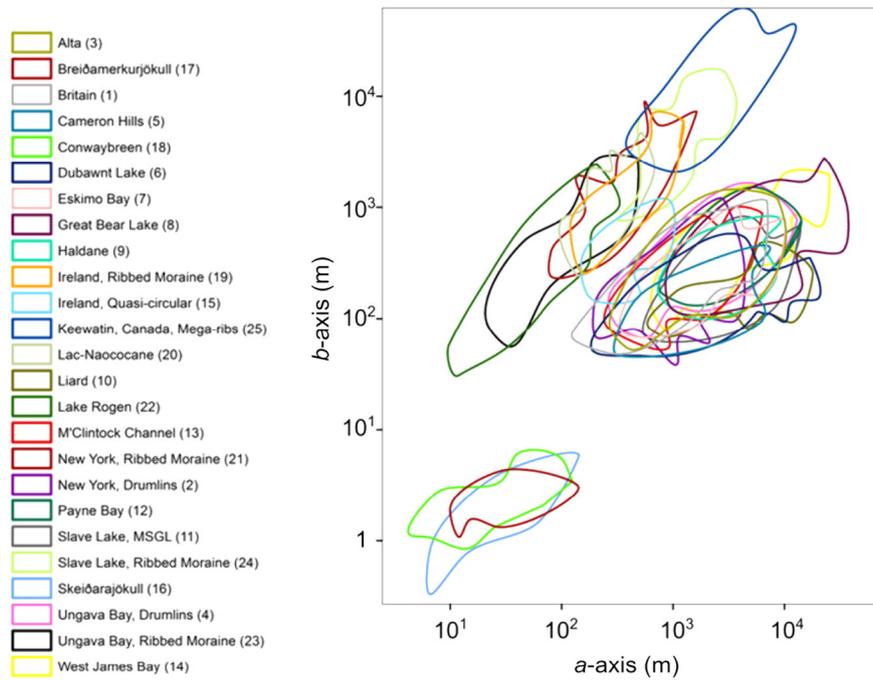|		Range (m)	Median (m)	10th percentile (m)	90th percentile (m)	Coefficient of variation
Flutes	*a*-Axis	138.1	30.5	12.9	68.4	0.6
	b-Axis	5.6	2.1	1.3	3.4	0.4
	Elongation	41.0	15.3	7.9	25.2	0.4
Megasubglacial ribs	*a*-Axis	11765.4	1980.4	1094.6	3706.4	0.6
	b-Axis	53940.1	9286.3	4283.4	17692.7	0.6
	Elongation	0.55	0.2	0.1	0.4	0.4
Ribbed Moraines	*a*-Axis	3683.6	196.9	61.2	606.5	0.9
	b-Axis	16749.8	701.1	260.1	1941.8	1.0
	Elongation	0.75	0.27	0.2	0.4	0.4
Circular Bedform	*a*-Axis	876.4	416.9	274.6	615.0	0.3
	b-Axis	1002.7	409.2	264.3	596.6	0.3
	Elongation	2.64	1.0	0.7	1.4	0.3
Drumlins	*a*-Axis	10602.1	603.5	323.4	1372.6	0.7
	b-Axis	1509.7	213.6	131.2	371.7	0.5
	Elongation	36.20	2.8	1.9	4.9	0.5
MSGLs	*a*-Axis	37268.2	1102.1	427.4	3912.9	1.2
	b-Axis	2725.8	150.1	81.7	479.2	0.9
	Elongation	131.62	6.4	4.0	12.9	0.8

Fig. 9. Outlines of the length and width of bedform scatter plots grouped by location. Locations are listed in Table 1. Note the overlap between locations, such that data from no single location is found to be unique.

correspond to morphological differences in the bedforms/landforms (e.g., Raukas and Tavast, 1994; Rattas and Piotrowski, 2003; Greenwood and Clark, 2010). As deformable sediment can accommodate accelerated ice flow (Alley et al., 1986), the glaciological and sedimentological properties of an ice mass can be interlinked. For example, where there is a boundary between a hard bedrock and soft deformable sediment, there is often a corresponding increase in bedform elongation, interpreted to

correspond to an acceleration in ice flow (e.g., Wellner et al., 2001; Ó Cofaigh et al., 2002). Therefore, given the complex interaction between ice flow and the nature of its underlying substrate, the exact influence of each of these two components can be rarely discerned.

The most commonly invoked glaciological control on subglacial bedform morphology is ice velocity. Ribbed moraines typically are found near ice divides or cold-based regions (Hättestrand, 1997;
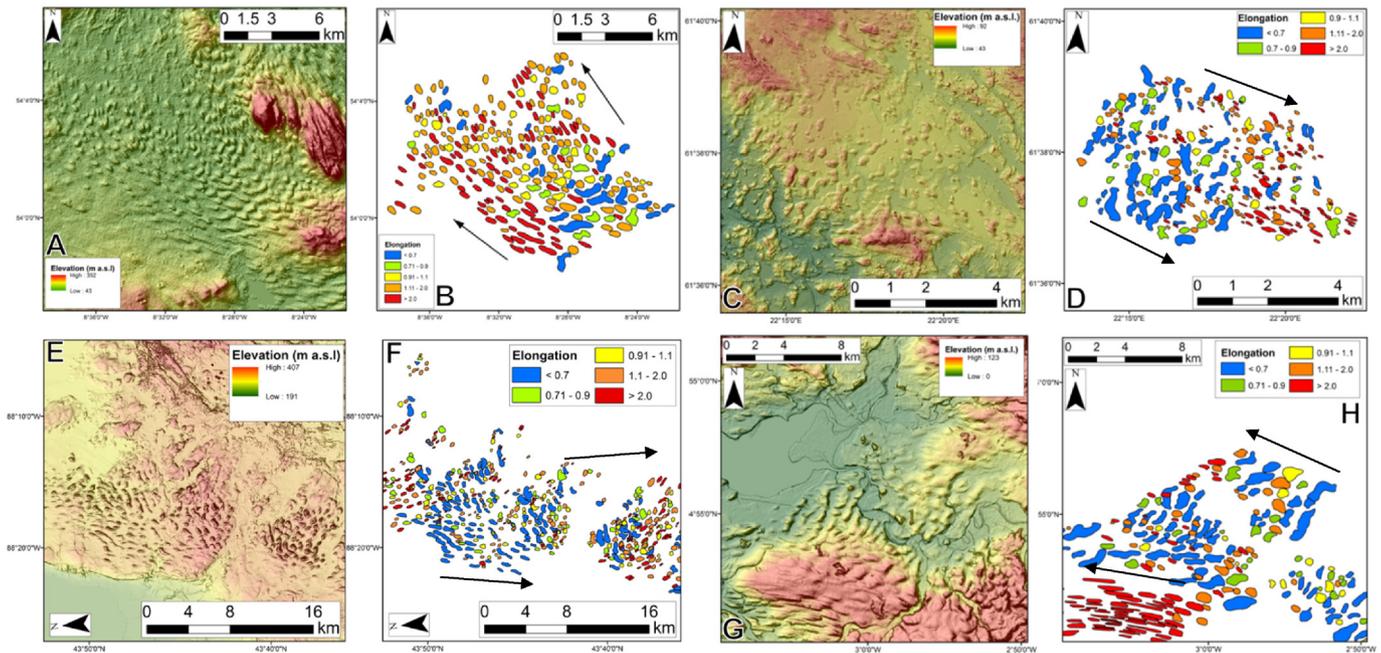

Fig. 10. Examples of spatial transitions between ribbed moraines and drumlins. Note how in each case, bedforms with no clear alignment to flow (elongation ratio of 0.9 to 1.1; yellow) were noted. (A) Hill-shaded SRTM DEM (30 m) and mapping (B) of bedforms in County Roscommon, Ireland. (C) 2 m LiDAR-derived DEM and mapping (D) of bedforms near Harjavalta, Finland. (E) Hill-shaded 2 m LiDAR DEM and mapping (F) of bedforms in Fon Du Lac County, Wisconsin, USA. (G) Hill-shaded NEXTMAP (5 m) DEM and mapping of bedforms (H) in Cumbria, UK. (For interpretation of the references to colour in this figure legend, the reader is referred to the web version of this article.)

Trommelen et al., 2014) or on ice-stream beds where they have been inferred to record deceleration immediately prior to ice stream shut-down (Stokes et al., 2008). This suggests slower ice flow is associated with their formation, even if the precise mechanisms are unknown. Drumlins are found farther away from ice divides and in the onset zones of palaeo (Stokes and Clark, 1999; Anderson and Fretwell, 2008) and contemporary ice streams (King et al., 2007), whereas more elongate subglacial lineations (MSGLs) have been associated with ice streams (Clark, 1993, 1994; Stokes and Clark, 1999; King et al., 2009; Spagnolo et al., 2014a). Ice velocity seems to be a prima-ry influence upon bedform orientation and elongation within and between ribs and lineations. Flutes have a separate morphology to other subglacial bedforms (Figs. 5–9). Thus, it is likely that they form under a separate set of boundary conditions or by a process dif-ferent to the larger bedforms.

The size and shape variations of subglacial bedforms appear to be predominately explicable in terms of position within the ice sheet and by variations in glaciological properties. In contrast, bedform sedimentary composition is found to be incredibly varied (overview of ribbed moraine in Hättestrand and Kleman, 1999; drumlins reviewed in Stokes et al., 2011, see references therein) and no simple match has been found between sediment properties and the various-ly named types. Sediment within bedforms can contain evidence of deposition (e.g., Dardis et al., 1984; Fisher and Shaw, 1992; Newman and Mickelson, 1994; Möller, 2010; Spagnolo et al., 2014b; Hopkins et al., 2016) and erosion (e.g., Boyce and Eyles, 1991; Kerr and Eyles, 2007; Ó Cofaigh et al., 2013), as well as several phases of development (Newman et al., 1990; Zelčs and Dreimanis, 1997). Thus, competing erosional and depositional processes are likely to occur at the ice-bed interface during bedform production (Hart, 1997). The bedform conundrum is that the order and simplic-ity in size and shape that we observe, and which tends to lead to pre-sumptions of a unifying process to create them, clashes with the complexity and variation found in the sedimentary properties, which tends to lead to suggestions of a whole range of different pro-cesses. We do not solve this problem here, but suggest that our data could be used as a test for any hypothesis or model of bedform for-mation, noting that the size and shape of bedforms as described here (Figs. 5–9) require explanation, as does their varied internal structure.

5. Conclusions

To test the hypothesis that subglacial bedforms comprise a size and shape continuum across the variously-named types, we analysed 96,900 measurements of subglacial bedform size and shape. The approach was to assess if bedforms vary continuously in size and shape, and thereby comprise a continuum, or whether gaps or jumps exist between the variously named types, indicating that they should be interpreted as discrete phenomena and therefore leading to the continuum hypothesis being rejected. Qualitative and quantitative (cluster) analyses of the data were employed to assess the degree to which separate populations exist. Although there is in-herent subjectivity in any type of cluster analysis, be it visual or quantitative, the convergence of results from our analyses leads us to the following conclusions:

- Subglacial flutes form a distinct cluster of narrower subglacial bedforms, clearly separable from other bedforms.
- Drumlins and MSGL are end members of a size and shape continuum of flow-aligned subglacial bedforms (subglacial lineations).
- Transverse subglacial bedforms belong to a subglacial rib continuum that spans ribbed moraine through to mega-ribbed moraine, with no justification found here for separate entities existing within this class.
- An underreported class of bedforms that are quasi-circular potentially bridge the more obvious continua of lineations and ribs suggesting

that a single subglacial continuum spanning ribs, quasi-circular forms, and lineations might exist. To test this possibility, further work on quasi-circular forms is required to increase the sample size and examine the range of scales at which they exist.

References

Aario, R., 1977. Classification and terminology of morainic landforms in Finland. Boreas 6 (2), 87–100.
Allen, J.R.L., 1968. The nature and origin of bed-form hierarchies. Sedimentology 10 (3), 161–182.
Alley, R.B., Blankenship, D.D., Bentley, C.R., Rooney, S., 1986. Deformation of till beneath ice stream B, West Antarctica. Nature 322, 57–59.
Amos, C.L., King, E.L., 1984. Bedforms of the Canadian eastern seaboard: a comparison with global occurrences. Mar. Geol. 57 (1), 167–208.
Anderson, J.B., Fretwell, L.O., 2008. Geomorphology of the onset area of a paleo-ice stream, Marguerite Bay, Antarctic Peninsula. Earth Surf. Process. Landf. 33 (4), 503–512.
Andreassen, K., Laberg, J.S., Vorren, T.O., 2008. Seafloor geomorphology of the SW Barents Sea and its glaci-dynamic implications. Geomorphology 97 (1), 157–177.
Ashley, G.M., 1990. Classification of large-scale subaqueous bedforms: a new look at an old problem—SEPM bedforms and bedding structures. J. Sediment. Res. 60 (1), 160–172.
Aylsworth, J.M., Shilts, W.W., 1989. Bedforms of the Keewatin ice sheet, Canada. Sedi-ment. Geol. 62 (2), 407–428.
Bouchard, M.A., 1989. Subglacial landforms and deposits in central and northern Quebec, Canada, with emphasis on Rogen moraines. Sediment. Geol. 62 (2), 293–308.
Boulton, G.S., 1976. The origin of glacially fluted surfaces—observations and theory. J. Glaciol. 17, 287–309.
Boulton, G.S., 1987. A theory of drumlin formation by subglacial sediment deformation. In: Menzies, J., Rose, J. (Eds.), Drumlin Symposium. Balkema, Rotterdam, pp. 25–80.
Boyce, J.I., Eyles, N., 1991. Drumlins carved by deforming till streams below the Laurentide ice sheet. Geology 19 (8), 787–790.
Briner, J.P., 2007. Supporting evidence from the New York drumlin field that elongate subglacial bedforms indicate fast ice flow. Boreas 36 (2), 143–147.
Brown, V.H., Stokes, C.R., O'Cofaigh, C., 2011. The glacial geomorphology of the North–West sector of the Laurentide Ice Sheet. J. Maps 7 (1), 409–428.
Carl, J.D., 1978. Ribbed moraine–drumlin transition belt, St. Lawrence Valley, New York. Geology 6 (9), 562–566.
Carling, P.A., 1999. Subaqueous gravel dunes. J. Sediment. Res. 69 (3).
Clark, C.D., 1993. Mega-scale glacial lineations and cross-cutting ice-flow landforms. Earth Surf. Process. Landf. 18 (1), 1–29.
Clark, C.D., 1994. Large-scale ice-moulding: a discussion of genesis and glaciological sig-nificance. Sediment. Geol. 91 (1), 253–268.
Clark, C.D., 1999. Glaciodynamic context of subglacial bedform generation and preserva-tion. Ann. Glaciol. 28 (1), 23–32.
Clark, C.D., Hughes, A.L., Greenwood, S.L., Spagnolo, M., Ng, F.S., 2009. Size and shape char-acteristics of drumlins, derived from a large sample, and associated scaling laws. Quat. Sci. Rev. 28 (7), 677–692.
Costello, W.R., Southard, J.B., 1981. Flume experiments on lower-flow-regime bed forms in coarse sand. J. Sediment. Res. 51 (3).
Cutts, J.A., Smith, R.S.U., 1973. Eolian deposits and dunes on Mars. J. Geophys. Res. 78 (20), 4139–4154.
Dardis, G.F., McCabe, A.M., Mitchell, W.I., 1984. Characteristics and origins of lee-side stratification sequences in late Pleistocene drumlins, Northern Ireland. Earth Surf. Process. Landf. 9 (5), 409–424.
Dionne, J.C., 1987. Tadpole rock (rock drumlin): a glacial stream moulded form. In: Menzies, J., Rose, J. (Eds.), Drumlin Symposium. Balkema, Rotterdam, pp. 149–159.
Dowling, T.P.F., Spagnolo, M., Möller, P., 2015. Morphometry and core type of streamlined bedforms in southern Sweden from high resolution LiDAR. Geomorphology 236, 54–63.
Dunlop, P., Clark, C.D., 2006a. Distribution of ribbed moraine in the Lac Naococane Region, Central Québec, Canada. J. Maps 2 (1), 59–70.
Dunlop, P., Clark, C.D., 2006b. The morphological characteristics of ribbed moraine. Quat. Sci. Rev. 25 (13), 1668–1691.
Dyke, A.S., Morris, T.F., Green, D.E.C., England, J., 1992. Quaternary geology of Prince of Wales Island, Arctic Canada. Geol. Surv. Can. Mem. 433, 142.
Ellwood, J.M., Evans, P.D., Wilson, I.G., 1975. Small scale aeolian bedforms. J. Sediment. Res. 45 (2), 554–561.

Engelhardt, H., Kamb, B., 1998. Basal sliding of ice stream B, West Antarctica. J. Glaciol. 44 (147), 223–230.

Ester, M., Kriegel, H.P., Sander, J., Xu, X., 1996. A density-based algorithm for discovering clusters in large spatial databases with noise. Kdd 96 (34), 226–231.

Estivill-Castro, V., 2002. Why so many clustering algorithms: a position paper. ACM SIGKDD Explorations Newsletter 4 (1), 65–75.

Evans, D.J., Twigg, D.R., 2002. The active temperate glacial landsystem: a model based on Breiðamerkurjökull and Fjallsjökull, Iceland. Quat. Sci. Rev. 21 (20), 2143–2177.

Fisher, T.G., Shaw, J., 1992. A depositional model for Rogen moraine, with examples from the Avalon Peninsula, Newfoundland. Can. J. Earth Sci. 29 (4), 669–686.

Greenwood, S.L., Clark, C.D., 2008. Subglacial bedforms of the Irish ice sheet. J. Maps 4 (1), 332–357.

Greenwood, S.L., Clark, C.D., 2010. The sensitivity of subglacial bedform size and distribution to substrate lithological control. Sediment. Geol. 232 (3), 130–144.

Greenwood, S.L., Kleman, J., 2010. Glacial landforms of extreme size in the Keewatin sector of the Laurentide Ice Sheet. Quat. Sci. Rev. 29 (15), 1894–1910.

Hart, J.K., 1995. Drumlin formation in southern Anglesey and Arvon, northwest Wales. J. Quat. Sci. 10 (1), 3–14.

Hart, J.K., 1997. The relationship between drumlins and other forms of subglacial glaciotectonic deformation. Quat. Sci. Rev. 16 (1), 93–107.

Hart, J.K., 1999. Identifying fast ice flow from landform assemblages in the geological record: a discussion. Ann. Glaciol. 28 (1), 59–66.

Hättestrand, C., 1997. Ribbed moraines in Sweden—distribution pattern and palaeoglaciological implications. Sediment. Geol. 111 (1), 41–56.

Hättestrand, C., Kleman, J., 1999. Ribbed moraine formation. Quat. Sci. Rev. 18 (1), 43–61.

Hess, D.P., Briner, J.P., 2009. Geospatial analysis of controls on subglacial bedform morphometry in the New York Drumlin Field—implications for Laurentide Ice Sheet dynamics. Earth Surf. Process. Landf. 34 (8), 1126–1135.

Hill, A.R., 1973. The distribution of drumlins in County Down, Ireland. Ann. Assoc. Am. Geogr. 63 (2), 226–240.

Hopkins, N.R., Evenson, E.B., Kodama, K.P., Kozlowski, A., 2016. An anisotropy of magnetic susceptibility (AMS) investigation of the till fabric of drumlins: support for an accretionary origin. Boreas 45 (1), 100–108.

Hughes, A.L., Clark, C.D., Jordan, C.J., 2010. Subglacial bedforms of the last British Ice Sheet. J. Maps 6 (1), 543–563.

Jackson, R.G., 1975. Hierarchical attributes and a unifying model of bed forms composed of cohesionless material and produced by shearing flow. Geol. Soc. Am. Bull. 86 (11), 1523–1533.

Jain, A.K., 2010. Data clustering: 50 years beyond K-means. Pattern Recogn. Lett. 31 (8), 651–666.

Johnson, M.D., Schomacker, A., Benediktsson, Í.Ö., Geiger, A.J., Ferguson, A., Ingólfsson, Ó., 2010. Active drumlin field revealed at the margin of Múlajökull, Iceland: a surge-type glacier. Geology 38 (10), 943–946.

Kargel, J.S., Strom, R.G., 1992. Ancient glaciation on Mars. Geology 20 (1), 3–7.

Kerr, M., Eyles, N., 2007. Origin of drumlins on the floor of Lake Ontario and in upper New York State. Sediment. Geol. 193 (1), 7–20.

King, E.C., Woodward, J., Smith, A.M., 2007. Seismic and radar observations of subglacial bed forms beneath the onset zone of Rutford Ice Stream, Antarctica. J. Glaciol. 53 (183), 665–672.

King, E.C., Hindmarsh, R.C., Stokes, C.R., 2009. Formation of mega-scale glacial lineations observed beneath a West Antarctic ice stream. Nat. Geosci. 2 (8), 585–588.

Kjær, K.H., Larsen, E., van der Meer, J., Ingólfsson, Ó., Krüger, J., Benediktsson, Í.Ö., Knudsen, C.G., Schomacker, A., 2006. Subglacial decoupling at the sediment/bedrock interface: a new mechanism for rapid flowing ice. Quat. Sci. Rev. 25 (21), 2704–2712.

Klages, J.P., Kuhn, G., Hillenbrand, C.D., Graham, A.G.C., Smith, J.A., Larter, R.D., Gohl, K., 2013. First geomorphological record and glacial history of an inter-ice stream ridge on the West Antarctic continental shelf. Quat. Sci. Rev. 61, 47–61.

Kleman, J., Glasser, N.F., 2007. The subglacial thermal organisation (STO) of ice sheets. Quat. Sci. Rev. 26 (5), 585–597.

Knight, J., McCarron, S.G., McCabe, A.M., 1999. Landform modification by palaeo-ice streams in east-central Ireland. Ann. Glaciol. 28 (1), 161–167.

Lancaster, N., 1988. Controls of eolian dune size and spacing. Geology 16 (11), 972–975.

Lancaster, N., 2013. Geomorphology of Desert Dunes. Routledge, p. 159.

Lane, T.P., Roberts, D.H., Rea, B.R., Ó Cofaigh, C., Vieli, A., 2015. Controls on bedrock bedform development beneath the Uummannaq Ice Stream onset zone, West Greenland. Geomorphology 231, 301–313.

Larter, R.D., Graham, A.G., Gohl, K., Kuhn, G., Hillenbrand, C.D., Smith, J.A., Deen, T.J., Livermore, R.A., Schenke, H.W., 2009. Subglacial bedforms reveal complex basal regime in a zone of paleo-ice stream convergence, Amundsen Sea embayment, West Antarctica. Geology 37 (5), 411–414.

Maclachlan, J.C., Eyles, C.H., 2013. Quantitative geomorphological analysis of drumlins in the Peterborough drumlin field, Ontario, Canada. Geografiska Annaler: Series A, Physical Geography 95 (2), 125–144.

Markgren, M., Lassila, M., 1980. Problems of moraine morphology: Rogen moraine and Blattnick moraine. Boreas 9 (4), 271–274.

McHenry, M., Dunlop, P., 2015. The subglacial imprint of the last Newfoundland Ice Sheet, Canada. J. Maps 1–22 (ahead-of-print).

Möller, P., 2010. Melt-out till and ribbed moraine formation, a case study from south Sweden. Sediment. Geol. 232 (3), 161–180.

Napieralski, J., Nalepa, N., 2010. The application of control charts to determine the effect of grid cell size on landform morphometry. Comput. Geosci. 36 (2), 222–230.

Newman, W.A., Mickelson, D.M., 1994. Genesis of Boston Harbor drumlins, Massachusetts. Sediment. Geol. 91 (1), 333–343.

Newman, W.A., Berg, R.C., Rosen, P.S., Glass, H.D., 1990. Pleistocene stratigraphy of the Boston Harbor drumlins, Massachusetts. Quat. Res. 34 (2), 148–159.

Ó Cofaigh, C., Pudsey, C.J., Dowdeswell, J.A., Morris, P., 2002. Evolution of subglacial bedforms along a paleo-ice stream, Antarctic Peninsula continental shelf. Geophys. Res. Lett. 29 (8), 41-1.

Ó Cofaigh, C., Stokes, C.R., Lian, O.B., Clark, C.D., Tulaczyk, S., 2013. Formation of megascale glacial lineations on the Dubawnt Lake Ice Stream bed: 2. Sedimentology and stratigraphy. Quat. Sci. Rev. 77, 210–227.

Ottesen, D., Dowdeswell, J.A., Rise, L., 2005. Submarine landforms and the reconstruction of fast-flowing ice streams within a large Quaternary ice sheet: the 2500-km-long Norwegian–Svalbard margin (57–80 N). Geol. Soc. Am. Bull. 117 (7–8), 1033–1050.

Punkari, M., 1984. The relations between glacial dynamics and the tills in the eastern part of the Baltic shield. In: Königsson, L.-K. (Ed.), Ten Years of Nordic Till Research, Striae. 20, pp. 49–54.

Radebaugh, J., Lorenz, R.D., Lunine, J.I., Wall, S.D., Boubin, G., Reffet, E., Kirk, R.L., Lopes, R.M., Stofan, E.R., Soderblom, L., Allison, M., Janssen, M., Paillou, P., Callahan, P., Spencer, C., The Cassini RADAR Team, 2008. Dunes on Titan observed by Cassini RADAR. Icarus 194 (2), 690–703.

Rattas, M., Piotrowski, J.A., 2003. Influence of bedrock permeability and till grain size on the formation of the Saadjärve drumlin field, Estonia, under an east-Baltic Weichselian ice stream. Boreas 32 (1), 167–177.

Raukas, A., Tavast, E., 1994. Drumlin location as a response to bedrock topography on the southeastern slope of the Fennoscandian Shield. Sediment. Geol. 91 (1), 373–382.

Reffet, E., du Pont, S.C., Hersen, P., Douady, S., 2010. Formation and stability of transverse and longitudinal sand dunes. Geology 38 (6), 491–494.

Rooney, S.T., Blankenship, D.D., Alley, R.B., Bentley, C.R., 1987. Till beneath ice stream B: 2. Structure and continuity. J. Geophys. Res. Solid Earth (1978–2012) 92 (B9), 8913–8920.

Rose, J., 1987. Drumlins as part of glacier bedform continuum. In: Menzies, J., Rose, J. (Eds.), Drumlin Symposium. Balkema, Rotterdamn, pp. 103–118.

Rose, J., Letzer, J.M., 1977. Superimposed drumlins. J. Glaciol. 18 (80), 471–480.

Rubin, D.M., Ikeda, H., 1990. Flume experiments on the alignment of transverse, oblique, and longitudinal dunes in directionally varying flows. Sedimentology 37 (4), 673–684.

Saha, K., Wells, N.A., Munro-Stasiuk, M., 2011. An object-oriented approach to automated landform mapping: a case study of drumlins. Comput. Geosci. 37 (9), 1324–1336.

Smith, M.J., Clark, C.D., 2005. Methods for the visualization of digital elevation models for landform mapping. Earth Surf. Process. Landf. 30 (7), 885–900.

Smith, M.J., Wise, S.M., 2007. Problems of bias in mapping linear landforms from satellite imagery. Int. J. Appl. Earth Obs. Geoinf. 9 (1), 65–78.

Smith, A.M., Murray, T., Nicholls, K.W., Makinson, K., Aðalgeirsdóttir, G., Behar, A.E., Vaughan, D.G., 2007. Rapid erosion, drumlin formation, and changing hydrology beneath an Antarctic ice stream. Geology 35 (2), 127–130.

Spagnolo, M., Clark, C.D., Hughes, A.L., Dunlop, P., Stokes, C.R., 2010. The planar shape of drumlins. Sediment. Geol. 232 (3), 119–129.

Spagnolo, M., Clark, C.D., Ely, J.C., Stokes, C.R., Anderson, J.B., Andreassen, K., Graham, A.G.C., King, E.C., 2014a. Size, shape and spatial arrangement of mega-scale glacial lineations from a large and diverse dataset. Earth Surf. Process. Landf. 39 (11), 1432–1448.

Spagnolo, M., King, E.C., Ashmore, D.W., Rea, B.R., Ely, J.C., Clark, C.D., 2014b. Looking through drumlins: testing the application of ground-penetrating radar. J. Glaciol. 60 (224), 1126–1134.

Stokes, C.R., Clark, C.D., 1999. Geomorphological criteria for identifying Pleistocene ice streams. Ann. Glaciol. 28 (1), 67–74.

Stokes, C.R., Clark, C.D., 2002. Are long subglacial bedforms indicative of fast ice flow? Boreas 31 (3), 239–249.

Stokes, C.R., Lian, O.B., Tulaczyk, S., Clark, C.D., 2008. Superimposition of ribbed moraines on a palaeo-ice-stream bed: implications for ice stream dynamics and shutdown. Earth Surf. Process. Landf. 33 (4), 593–609.

Stokes, C.R., Spagnolo, M., Clark, C.D., 2011. The composition and internal structure of drumlins: complexity, commonality, and implications for a unifying theory of their formation. Earth Sci. Rev. 107 (3), 398–422.

Stokes, C.R., Fowler, A.C., Clark, C.D., Hindmarsh, R.C., Spagnolo, M., 2013a. The instability theory of drumlin formation and its explanation of their varied composition and internal structure. Quat. Sci. Rev. 62, 77–96.

Stokes, C.R., Spagnolo, M., Clark, C.D., Ó Cofaigh, C., Lian, O.B., Dunstone, R.B., 2013b. Formation of mega-scale glacial lineations on the Dubawnt Lake Ice Stream bed: 1. Size, shape and spacing from a large remote sensing dataset. Quat. Sci. Rev. 77, 190–209.

Storrar, R., Stokes, C.R., 2007. A glacial geomorphological map of Victoria Island, Canadian Arctic. J. Maps 3 (1), 191–210.

Trommelen, M., Ross, M., 2010. Subglacial landforms in northern Manitoba, Canada, based on remote sensing data. J. Maps 6 (1), 618–638.

Trommelen, M.S., Ross, M., Ismail, A., 2014. Ribbed moraines in northern Manitoba, Canada: characteristics and preservation as part of a subglacial bed mosaic near the core regions of ice sheets. Quat. Sci. Rev. 87, 135–155.

Waller, R.I., Van, D.A.T., Knudsen, Ó., 2008. Subglacial bedforms and conditions associated with the 1991 surge of Skeiðarárjökull, Iceland. Boreas 37 (2), 179–194.

Wellner, J.S., Lowe, A.L., Shipp, S.S., Anderson, J.B., 2001. Distribution of glacial geomorphic features on the Antarctic continental shelf and correlation with substrate: implications for ice behavior. J. Glaciol. 47 (158), 397–411.

Wilson, I.G., 1973. Ergs. Sediment. Geol. 10 (2), 77–106.

Winsborrow, M., Clark, C.D., Stokes, C.R., 2004. Ice streams of the Laurentide ice sheet. Géog. Phys. Quatern. 58 (2–3), 269–280.

Worman, S.L., Murray, A.B., Littlewood, R., Andreotti, B., Claudin, P., 2013. Modeling emergent large-scale structures of barchan dune fields. Geology 41 (10), 1059–1062.

Zelčs, V., Dreimanis, A., 1997. Morphology, internal structure and genesis of the Burtnieks drumlin field, Northern Vidzeme, Latvia. Sediment. Geol. 111 (1), 73–90.